ELSEVIER

Biophysical Chemistry 107 (2004) 7–17

Biophysical Chemistry

www.elsevier.com/locate/bpc

Dual role of sequence-dependent DNA curvature in nucleosome stability: the critical test of highly bent *Crithidia fasciculata* DNA tract

Anita Scipioni[a], Sabrina Pisano[b], Claudio Anselmi[a], Maria Savino[b], Pasquale De Santis[a,*]

[a]*Dipartimento di Chimica, Università di Roma 'La Sapienza', 00185 Rome, Italy*
[b]*Dipartimento di Genetica e Biologia Molecolare, Università di Roma 'La Sapienza', 00185 Rome, Italy*

Received 10 July 2003; received in revised form 22 July 2003; accepted 22 July 2003

Abstract

In spite of the knowledge of the nucleosome molecular structure, the role of DNA intrinsic curvature in determining nucleosome stabilization is still an open question. In this paper, we describe a general model that allows the prediction of the nucleosome stability, tested on 83 different DNA sequences, in surprising good agreement with the experimental data, carried out in ours as well as in many other laboratories. The model is based on the dual role of DNA curvature in nucleosome thermodynamic stabilization. A critical test is the evaluation of the nucleosome free energy relative to a *Crithidia fasciculata* kinetoplast DNA fragment, which represents the most curved DNA found so far in biological systems and, therefore, is generally believed to form a highly stable nucleosome.

Keywords: Nucleosome stability; DNA curvature; DNA flexibility; Theoretical predictions

1. Introduction

Static and dynamic curvature is involved in fundamental DNA functions such as transcription, recombination and chromatin organization. Their role is associated to the recognition mechanisms involving proteins as a relevant factor in the differential stabilization of DNA–protein complexes, like nucleosomes.

Nucleosome is the DNA association complex with the histone octamer and represents the elemental unit of chromatin. Its structure is characterized by a flat solenoid-like structure in which a DNA tract of 145 bp is wrapped around the histone core with a pseudo-dyad symmetry [1,2]. Recently, a 1.9 Å resolution electron density map of the nucleosome was obtained [3], which confirms the main features of the previously proposed structure [4]. However, the deeper knowledge of the molecular structure, which reveals a large mass of details of both DNA and the protein core, provides a dramatic image of the great complexity of the preferential nucleosome positioning along DNA. Nevertheless, it is generally accepted that positioning and stability of nucleosomes along genome DNAs can be considered a sequence-dependent property, but to what extent DNA sequences play

*Corresponding author. Tel./fax: +39-06-4453827.
E-mail address: pasquale.desantis@uniroma1.it (P. De Santis).

0301-4622/04/$ - see front matter © 2003 Elsevier B.V. All rights reserved.
doi:10.1016/S0301-4622(03)002140-X

a role in nucleosome positioning is still considered an open question.

Competitive reconstitution experiments allow the determination of the differential thermodynamic nucleosome affinity along a DNA sequence, providing a sound basis for discovering the sequence effects on nucleosome stability [5–21]. Several authors have made attempts to find the sequence features that enhance or, on the contrary, reduce the stability of nucleosomes.

The original hypothesis was that intrinsically curved DNA, characterized by phased sequences of AA·TT dinucleotide steps, could have a large propensity to form nucleosomes. This is consistent with the finding about the preferential distribution of such sequences facing towards the histone core [22]. However, a complex role of curvature emerged from these investigations. Shrader and Crothers [5,6] found that some intrinsically curved DNAs, which were supposed to form highly stable nucleosomes, surprisingly showed lower affinity for the histone octamer than relatively straight DNAs with similar sequences. DNAs isolated in the mouse genome, characterized by runs of three or four adenine-phased residues, extensive CA repeats, and TATA tetranucleotides, form very stable nucleosomes despite their low integral curvature [11]. Furthermore, SELEX experiments, carried out with a large pool of random DNA fragments, allowed the isolation of individuals having the highest histone affinity obtained so far. They were characterized by relatively low curvature [13].

Aside DNA curvature implications, an alternative point of view was proposed, which tries to explain the stability of the DNA–histone association as due to few specific DNA sites, which some authors localized nearby the nucleosome dyad axis [5,6,22–29].

Recently, we have developed a statistical mechanic model to derive the differential affinity between DNA and histones from the sequence-dependent curvature and flexibility [30,31]. We evaluated the equilibrium constant of the competitive nucleosome reconstitution in terms of thermodynamic and structural parameters of the dinucleotide steps adopting first-order elasticity to calculate the pertinent canonical partition functions involved in the nucleosome formation. The theoretical free-energy values so obtained showed a satisfactory agreement with the experimental data for a number of DNAs but major deviations for others. This disagreement, however, was positively correlated ($R=0.98$) with the DNA effective curvature, $\langle A_f \rangle$, which represents in modulus and phase the extent of similarity between the curvature of the free and the nucleosomal DNA. This strongly indicated the existence of a curvature-dependent contribution to the free energy, which appears to destabilize the nucleosome. This was interpreted as due to the groove contractions in intrinsically curved free DNAs, which stabilizes the water spine and counter-ion interactions [32–39], adding a further energy cost to the nucleosome formation, where a part of these free energy contributions is lost and substituted by the DNA–histone moiety interactions.

Therefore, the intrinsic curvature results to play two opposite roles in nucleosome formation: one stabilizing the nucleosome by reducing the elastic energy required to distort a DNA tract in the nucleosome structure; the other, apparently related to the curvature of the DNA free form, reducing the affinity with histone octamer. Such a dual role clearly appears when the experimental free energy of a homogeneous pool of DNA fragments [5,6] of close length and base composition is reported vs. the free DNA average effective curvature $\langle A_f \rangle$ [31]. The plot shows a free energy minimum for an average curvature of approximately 1.5 rad, which confirms the dual role of the curvature in the nucleosome stability; as a consequence, higher intrinsic curvature is a destabilizing factor of nucleosomes as well as low curvature, at least in the analyzed range.

Extrapolating the model to high curvature leads to the prediction that highly bent DNAs should form relatively unstable nucleosomes, contrary to the generally accepted opinions. Therefore, a critical test for the validity of the model is the evaluation of the histone affinity of the well-known highly curved tract of *Crithidia fasciculata* kinetoplast DNA [40].

Crithidia DNA fragment is characterized by in-phase repetitions of 4–5 AA·TT dinucleotide steps facing towards the histone surface. The direct

electron microscopy and atomic force microscopy (AFM) visualization [41,42] and the high PAGE retardation (Fig. 1) prove its high curvature. As a result, accordingly to generally accepted nucleosome model [24], it should be an optimum in nucleosome formation. On the contrary, we report in this paper that Crithidia DNA fragment has a high nucleosome-formation free energy, comparable with that of telomeres, the least stable nucleosomes found so far in eukaryotic genomes [14,19,21].

2. Materials and methods

2.1. Experimental

The 223 bp Crithidia fragment, with sequence

GATCCCGCCT AAAATTCCAA CCGAAAATCG CGAGGTTACT TTTTTGGAGC
CCGAAAACCA CCCAAAATCA AGGAAAAATG GCCAAAAAAT GCCAAAAAAT
AGCGAAAATA CCCCGAAAAT TGGCAAAAAT TAACAAAAAA TAGCGAATTT
CCCTGAATTT TAGGCGAAAA AACCCCCGAA AATGGCCAAA AACGCACTGA
AAATCAAAAT CTGAACGTCT CGG

containing the original Crithidia 211 curved tract insert [40], was prepared from Crithidia kinetoplast minicircle, after insertion in the plasmid *p*PK 201/cat and digestion with BamH1. Synthesis, multimerization and cloning of 222 bp *Homo sapiens* telomeric sequence were performed as previously described [12]. The 159 bp sequence TAND-1 was a gift of Andrew Travers.

The procedure used for the competitive reconstitution was that of Shrader and Crothers [5] with minor modifications. Three micrograms of H5-depleted polynucleosome, obtained from chicken erythrocyte, were mixed with 30 ng of radiolabelled 223 bp Crithidia fragment and 3 μg (R_3), 5 μg (R_5) and 7 μg (R_7) of sonicated calf thymus DNA as competitor in 6 μl of 0.9 M NaCl, 10 mM Tris–HCl pH 8.0, 1 mM EDTA pH 8.0 and 0.1% Nonidet P40. After incubation at room temperature for 30 min, the salt concentration was lowered to 50 mM NaCl, step by step with addition of the same buffer without NaCl. Samples were then resolved on 5% acrylamide gel in 0.5× TBE buffer. The relative quantities of the reconstituted and free DNA were assayed by scanning dried gels with Instant Imager (Packard). The free energy values were obtained from three ratios with different competitor amounts, measured at least in three separate experiments and the results obtained were averaged.

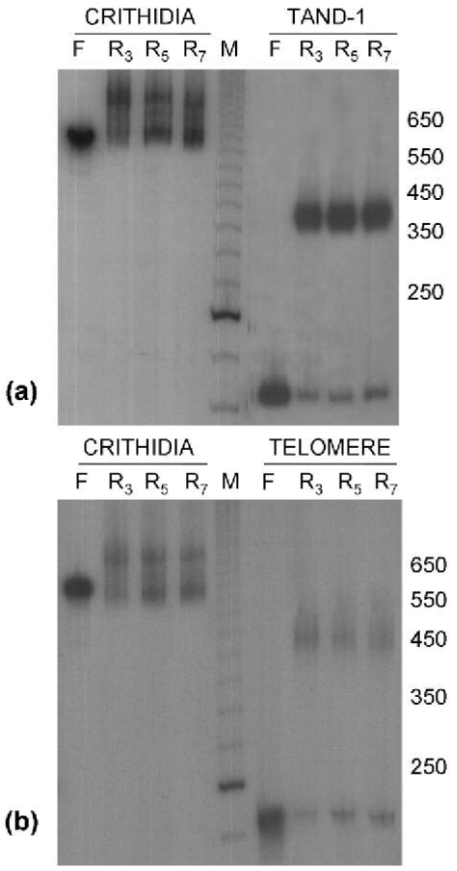

Fig. 1. Competitive nucleosome reconstitution assay. An example of nucleosome competitive reconstitution experiment of 223 bp Crithidia fragment compared with (a) 159 bp TAND-1 [19,22] and (b) 222 bp *H. sapiens* telomeric DNA fragment.

2.2. Theoretical evaluation of the nucleosome stability

If $\Delta G(k)$ represents the nucleosome reconstitution free-energy difference of the kth DNA tract with $L=145$ bp along a sequence with N bp, the free energy per mole of nucleosome, ΔG, pertinent to the whole DNA is

$$\beta\Delta G = -\ln \sum_{k=L/2}^{N-L/2} \exp[-\beta\Delta G(k)] \qquad (1)$$

where β is $1/RT$. The exponential term represents the equilibrium constant pertinent to the nucleosome reconstitution of the kth DNA tract.

The relation with the pertinent canonical partition functions allows us to write the nucleosome reconstitution free-energy difference as

$$\beta\Delta G(k) = -\ln \frac{Q_n(k)}{Q_n^*} + \ln \frac{Q_f(k)}{Q_f^*} \quad (2)$$

where $Q_n(k)$ is the configurational canonical partition function of the kth nucleosomal DNA tract along the sequence; $Q_f(k)$ is that relative to the corresponding free DNA and Q_n* and Q_f* are those pertinent to an ideal standard intrinsically straight DNA with a random sequence. The partition functions of the remaining DNA tracts not involved in the kth nucleosome are considered in a first approximation equivalent to those of the free DNA and cancel in the ratio. We evaluated the elastic contributions to the partition functions, related to the sum of the bending and twisting energies necessary to distort the intrinsic structure of the kth DNA tract in the nucleosomal form. Assuming first order elasticity we obtained

$$\beta\Delta G_{el}(k) = \beta\Delta E_{el}^{\circ}(k) - \frac{3}{2}L \ln \left\langle \frac{T}{T^*} \right\rangle + Z - \ln J_0(iZ) \quad (3)$$

where $\Delta E_{el}^{\circ}(k)$ is the minimum elastic energy required to distort the kth tract of L bp in the nucleosomal form; $\langle T/T^* \rangle$ is the average normalized dinucleotide empirical melting temperature of the kth DNA tract, which suitably represents the DNA differential rigidity, as recently supported by the analysis of DNA images by AFM [43,44]; Z is equal to $(\beta b/L)\langle T/T^* \rangle A_n A_f$, where A_n and A_f are the Fourier transform amplitudes of frequency -0.17 of the nucleosome and the free DNA curvature function along the L bp tract of the sequence. It is worth noting that $A_n A_f$ represents the correlation between the curvature of the nucleosomal DNA and that of the free form, according to the convolution theorem; finally, $J_0(iZ)$ is the Bessel function of the imaginary argument Z. The logarithm of this term corresponds to the average contribution to the free energy due to the fluctuations of the double-helix phasing in the nucleosomal structure.

$\Delta E_{el}^{\circ}(k)$ is evaluated as

$$\Delta E_{el}^{\circ}(k) = \frac{b^*}{2L} \left\langle \frac{T}{T^*} \right\rangle (A_n - A_f)^2 + \frac{t^*}{2L} \times \left\langle \frac{T}{T^*} \right\rangle [2\pi\Delta \mathrm{Tw}(k)]^2 \quad (4)$$

where b* and t* are the apparent bending and twisting force constants for a standard DNA and $\Delta\mathrm{Tw}(k)$ represents the twisting number difference between the nucleosome and the free kth DNA tract. The latter term was evaluated imposing a DNA periodicity of 10.2 bp per turn according to the experimental evidence [3,4].

It is worth noting that the ground-state elastic energy is calculated in terms of the squared difference between the Fourier terms, A_n and A_f. On the basis of the Parseval's equality [45], this corresponds to distort the global shape of the free DNA tract involved in the nucleosome formation, leaving the DNA local features practically invariant.

Alternatively, it is possible to evaluate the free energy pertinent to each nucleosome position along DNA, by constraining its dyad axis to lie on the pseudo-dyad axis in the large groove of the successive base pairs according to the X-ray structure. In this case, the logarithm of the Bessel function in Eq. (3) is replaced by a periodic function of the angle between the directions toward which effective intrinsic curvature points, and the major groove axis.

$$\beta\Delta G_{el}(k) = \beta\Delta E^{\circ}(k) - \frac{3}{2}L \ln \left\langle \frac{T}{T^*} \right\rangle + Z - Z\cos\varphi \quad (5)$$

Eq. (5) produces an evident tenfold periodicity in the trend of the nucleosome stability along a DNA sequence, especially for curved tracts, in which the bending energy differences between in-phase and out-of-phase nucleosomes are dramatic. However, as in the partition function, nucleosomes

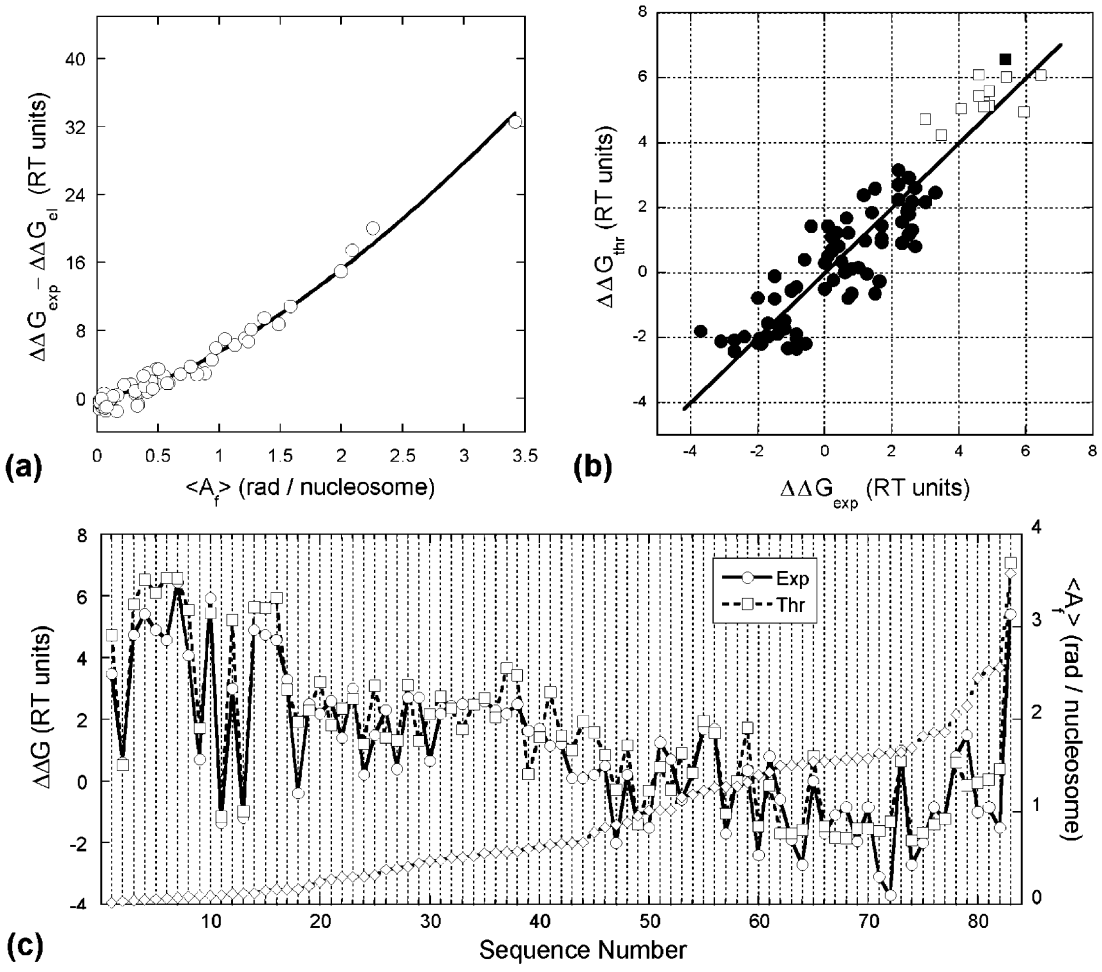

Fig. 2. (a) Deviations between the experimental and theoretical (elastic) nucleosome reconstitution free energy for the whole pool of the investigated DNAs as a function of the intrinsic effective curvature, represented by the average Fourier amplitude, $\langle A_f \rangle$. (b) Comparison between theoretical and experimental nucleosome reconstitution free energies for the Crithidia fragment (■), the telomeres (□) and the other sequences (○) reported in Table 1. Data are related to the TG pentamer as a standard [5,6]. Values are reported in *RT* units (1 $RT = 0.59$ kcal/mol at room temperature). (c) Comparison between theoretical (□) and experimental (○) nucleosome reconstitution free energies for the whole set of DNA fragments reported in Table 1, sorted according to increasing curvature, $\langle A_f \rangle$ (◇). Connecting lines are guides for the eye and have no physical meaning. DNA tracts are identified by the same numbers reported in Table 1.

are weighted by the inverse of the exponential of the free energy, those characterized by low bending energy count much more than the others. Therefore, despite the absolute values given by Eqs. (3) and (5) being slightly different, the predicted relative nucleosome stability results practically unaffected.

3. Results

Fig. 1 illustrates two examples of nucleosome competitive reconstitution experiments of 223 bp Crithidia fragment compared with TAND-1 [19,22] and 222 bp *H. sapiens* telomeric DNA fragments. Incidentally, it is interesting to note the different

Table 1
The whole set of DNA fragments, ordered by increasing value of curvature, $\langle A_f \rangle$

N #	Sequence	Reference	$\langle A_f \rangle$ (rad/nucl)	$\Delta\Delta G_{exp}$ (kcal/mol)
1	*H. sapiens* telomere (458 bp)	[21]	0.02	2.05
2	CGG_{74}	[8]	0.04	0.34
3	*H. sapiens* telomere (254 bp)	[19]	0.04	2.80
4	*H. sapiens* telomere (192 bp)	[19]	0.06	3.20
5	*H. sapiens* telomere (218 bp)	Personal communication	0.06	2.90
6	*B. mori* telomere	[19]	0.07	2.70
7	*T. termophila* telomere	[19]	0.08	3.80
8	*A. thaliana* telomere (236 bp)	[19]	0.09	2.40
9	CGG^{13}	[8]	0.10	0.42
10	*S. cerevisiae* telomere	[19]	0.10	3.50
11	CTG^{62}	[7]	0.10	−0.80
12	*K. lactis* telomere	[21]	0.12	1.78
13	CTG^{55}	[7]	0.12	−0.71
14	*H. sapiens* telomere (222 bp)	This paper	0.12	2.90
15	*C. reinhardtii* telomere	[19]	0.15	2.80
16	*A. thaliana* telomere (195 bp)	[19]	0.17	2.75
17	34	[6]	0.17	2.00
18	CTG^{10}	[8]	0.17	−0.24
19	5S rDNA	[21]	0.20	1.50
20	TRGC	[5]	0.25	1.30
21	20	[6]	0.28	1.55
22	BADSECS-2	[16]	0.30	0.84
23	AOUT	[6]	0.30	1.80
24	CAG-runs-CAG	[11]	0.30	0.12
25	19	[6]	0.32	0.90
26	*X. borealis* 5S	[15]	0.38	1.35
27	5S RNA gene	[8]	0.40	0.25
28	TAND-1	[19,22]	0.41	2.00
29	22	[6]	0.45	1.60
30	NoSecs-1	[11]	0.47	0.40
31	IGC	[6]	0.48	1.30
32	TGGA-3	[16]	0.51	1.47
33	TGGA-2	[16]	0.51	1.50
34	TGA	[16]	0.53	1.50
35	EXGC	[6]	0.55	1.55
36	TGGA-1	[16]	0.56	1.38
37	KlCEN2	[20]	0.57	1.30
38	KlCEN3	[20]	0.58	1.50
39	5S rDNA dimer	[21]	0.60	0.95
40	BADSECS-1	[16]	0.62	1.02
41	SCEN6	[15]	0.65	0.70
42	EXAT	[6]	0.66	0.70
43	H4 ΔCTG	[7]	0.67	0.04
44	Mouse minor satellite	[11]	0.67	0.06
45	H4 ΔCTG/CGG	[7]	0.78	0.12
46	CA-runs-CA-1	[11]	0.84	0.30
47	Histone H4 gene	[7]	0.86	−1.21
48	A-tracts A-1	[11]	0.89	0.12
49	618	[13]	0.96	−0.83
50	47	[17]	1.02	−0.89
51	ANISO	[6]	1.02	0.75
52	FIN	[6]	1.02	0.42
53	TATA-tetrads-TATA	[11]	1.16	−0.35

Table 1 *(Continued)*

N #	Sequence	Reference	$\langle A_f \rangle$ (rad/nucl)	$\Delta\Delta G_{exp}$ (kcal/mol)
54	ANNA	[6]	1.19	0.15
55	KlCEN4	[20]	1.23	1.00
56	KlCEN1	[20]	1.27	1.00
57	57	[17]	1.27	−1.01
58	TG	[5]	1.28	0
59	KlCEN1	[15]	1.32	0.21
60	67 fragment 9	[18]	1.40	−1.42
61	IAT	[6]	1.43	0.50
62	67 fragment 2	[18]	1.50	−0.35
63	67 fragment 6	[18]	1.51	−1.12
64	67	[17]	1.52	−1.60
65	GT	[5]	1.54	0.00
66	67 fragment 8	[18]	1.55	−1.01
67	67 fragment 5	[18]	1.56	−0.65
68	67 fragment 4	[18]	1.57	−0.50
69	67 fragment 7	[18]	1.58	−1.15
70	67 fragment 3	[18]	1.58	−0.50
71	67 fragment 10	[18]	1.63	−1.84
72	61 fragment 13	[18]	1.64	−2.19
73	TIATR	[6]	1.64	0.60
74	77	[17]	1.69	−1.60
75	61 fragment 12	[18]	1.82	−1.18
76	61	[17]	1.86	−0.50
77	56	[17]	1.86	−0.71
78	AEXT	[6]	2.06	0.50
79	TTT	[6]	2.15	0.90
80	51	[17]	2.45	−0.59
81	53	[17]	2.53	−0.50
82	20	[17]	2.56	−0.89
83	Crithidia fragment (223 bp)	This paper	3.58	3.20

PAGE mobility of Crithidia and the telomeric DNA fragments associated with the histones. They contain practically the same base pair number, but are characterized by curved and straight residual free DNA tracts and, as a consequence, by a different electrophoretic behavior. It should be noted that from the first lanes of Fig. 1a and b, which represent the Crithidia free DNA, was obtained a PAGE retardation factor equal to 2.8, in agreement with our model [46] (data not shown).

The thermodynamic association constants of the Crithidia fragment nucleosome results equal to $\Delta\Delta G = 3.2 \pm 0.3$ kcal/mol. It is very similar to that of the 222 bp *H. sapiens* telomere nucleosome, equal to $\Delta\Delta G = 2.9 \pm 0.3$ kcal/mol, which shows one of the lowest stability constants in the literature (Table 1), substantially lower than that of TAND-1, which represents the average stability of chicken erythrocyte nucleosomes. Both experimental values of the free-energy differences are relative to the TG pentamer [5,6].

These values are reported in Table 1 and compared with the other experimental free energy values available in the literature. They constitute a pool of 83 DNA tracts. Such a large set of sequences was used to reformulate the contribution assigned to water and counter-ion interactions in terms of effective curvature.

The free energy differences between experimental and theoretical elastic data were fitted with a good correlation ($R = 0.99$) by a function, which can be conveniently expressed as $4.5\langle A_f \rangle^{1.5}$ in *RT* units (Fig. 2a). It should be noted that the slight modification with respect to the former formulation does not sensitively change the previously obtained theoretical results.

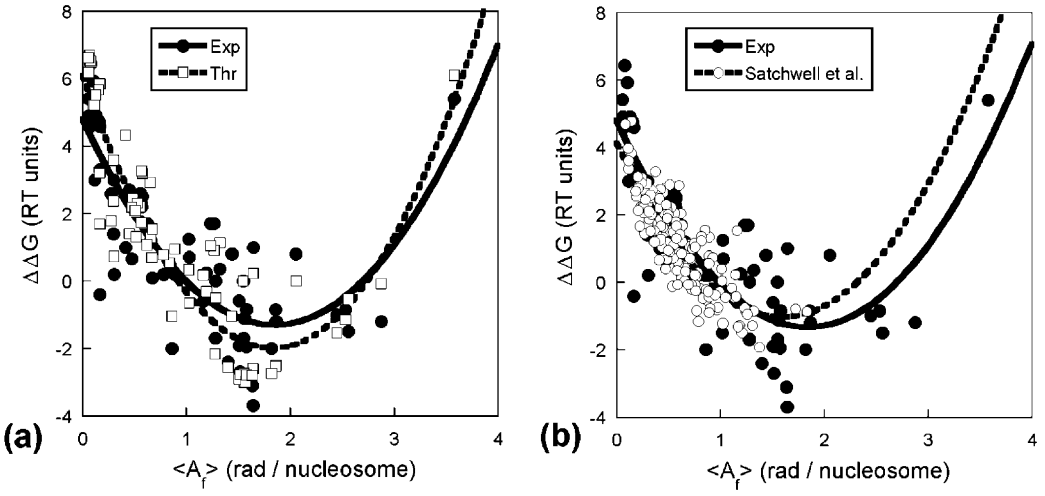

Fig. 3. (a) Experimental (●) and theoretical (□) nucleosome reconstitution free energy vs. the effective curvature, $\langle A_f \rangle$, for a subset of DNA fragments (sequence numbers: 4–7, 10, 12, 14–18, 21–24, 29–38, 40–48, 50–73, 75–78, 80–83) characterized by a close range of length (160–230 bp). (b) Comparison between the same experimental data (●) and the theoretical nucleosome reconstitution free energy of the set of chicken erythrocytes nucleosome cores studied by Satchwell et al. [22] (○) as a function of the effective curvature, $\langle A_f \rangle$.

Fig. 2b illustrates the comparison between the experimental and theoretical free-energy values of the whole set of 83 DNA tracts in Table 1, 35 more of those reported in our previous papers [30,31]. Data display a good linear correlation ($R = 0.92$). Fig. 2c shows the same data in Fig. 2b, sorted by increasing curvature. In spite of the apparent favorable conditions (high curvature and convenient distribution towards the histone core of the AA·TT steps), Crithidia DNA shows a low thermodynamic association constant, similar to the telomeric ones, in agreement with the prediction.

To illustrate the dual role of curvature, Fig. 3a reports the nucleosome competitive reconstitution free energy trend vs. the effective curvature of a subset of DNA tracts characterized by a close range of length (160–220 bp). Similar parabolic functions, with a minimum localized at the TG pentamer curvature, interpolate both the experimental and theoretical data. The substantial agreement between experimental and theoretical free energy data allows us to plot the theoretical results of the whole pool of 177 nucleosomal cores studied by Satchwell et al. [22]. They were obtained by digesting with endonuclease, cloning and sequencing the chicken erythrocyte chromatin. Fig. 3b shows that also this biologically significant sampling of nucleosomal DNAs is interpolated by practically the same function that fits the experimental data in Table 1, when plotted vs. the effective curvature.

4. Discussion

Despite the complexity of the nucleosome structure, which involves a large number of differential interactions between DNA and the histone core, our model appears to be surprisingly capable of predicting the sequence-dependent free energy of nucleosome formation, as shown by the good agreement between experimental and calculated data of more than 80 different DNA sequences, studied in our as well as in many other research groups. A critical test of the model is the relative low stability of the nucleosome of *Crithidia fasciculata* generally considered as the most curved natural DNA. An alternative explanation of such a low stability could be related to possible increased rigidity of the relatively long AA·TT repeating tracts. However, AFM results seem to

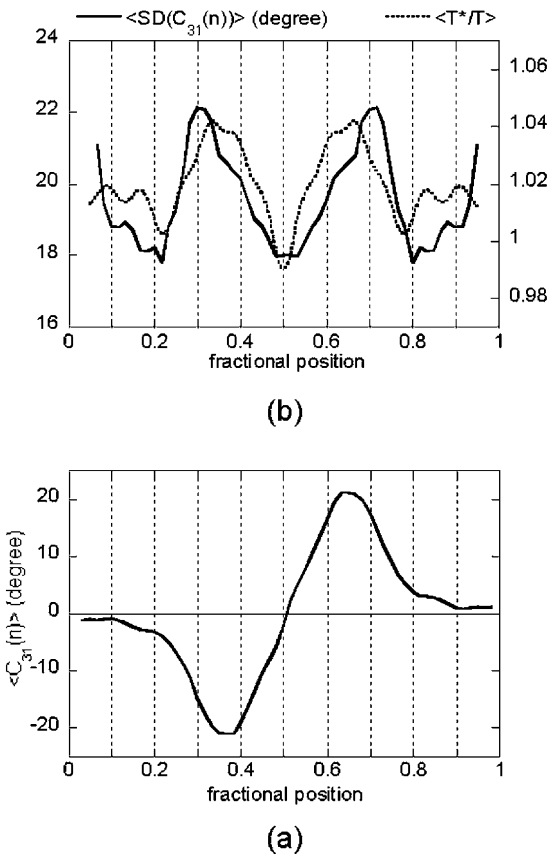

Fig. 4. (a) Curvature profile obtained by averaging the curvatures of a large ensemble of AFM images of a palindromic DNA construct containing the Crithidia fragment. (b) Flexibility profile, as evaluated from the curvature dispersion of the AFM images, with the normalized melting temperature profile adopted to represent the sequence-dependent differential flexibility superimposed. Curvature and flexibility profiles are given for recurrent tracts of 31 bp.

exclude such a hypothesis. In fact, Fig. 4a illustrates the curvature profile obtained by averaging the curvatures of a large ensemble of DNA AFM images of a palindromic construct containing the Crithidia fragment, as reported in a previous paper [47]. It permits a direct comparison with low curved adjacent DNA tracts. Fig. 4b shows the corresponding experimental flexibility profile, as evaluated from the curvature dispersion of the AFM images, with the normalized melting temperature profile adopted to represent the sequence-dependent differential flexibility superimposed. It clearly demonstrates the higher flexibility of the Crithidia tracts with respect to the adjacent canonical DNA tracts and the satisfactory melting temperature representation.

Therefore, we advance the conclusion that the intrinsic curvature is the main factor that controls nucleosome stability and, consequently, nucleosome positioning. It produces two opposite effects: it decreases the distortion energy of the free DNA tract necessary to assume the nucleosomal shape and increases the free-energy cost, corresponding to releasing a part of the water spine and counterions, consequent to the nucleosome formation.

As a matter of fact, the obtained results show that DNA mechanical properties, as averages of the sequence dinucleotide steps, are the main determinants of the stability and, probably, the kinetics of DNA–histones association process. The latter issue is a speculative consequence of our findings, which suggest that the rate-determining step in nucleosome formation is the transformation of the DNA curvature of the free state in that of the nucleosomal state.

The good results obtained prompted us to investigate the phasing and the translational positioning of nucleosomes along large DNA tracts. Also at this higher structural level, we assume that the interactions between the nucleosomes along the DNA are not specific and their packing mainly depends on the phasing of the nucleosomes. Attempts are in progress to predict the best nucleosome packing in genome tracts from nucleosome sequence. In the present post-genomic era, when the known DNA sequences are accumulating in the data banks, the need of translating the available information into functional elements is becoming even more crucial. Nucleosome positioning by means of free-energy predictions points toward such a direction.

Acknowledgments

The authors would like to thank Andrew A. Travers for the sequences of the 177 chicken erythrocyte nucleosome cores, and Beatrice Sampaolese and Raffaella Paparcone for helping in reconstitution experiments and in calculations.

This work was supported by 'Progetto 60% Ateneo' of University 'La Sapienza', MURST, Progetti di Ricerca di Interesse Nazionale 2001–2003, and by Istituto Pasteur, Fondazione Cenci-Bolognetti.

References

[1] A. Klug, D. Rhodes, J. Smith, T.J. Finch, J.O. Thomas, A low resolution structure for the histone core of the nucleosome, Nature 287 (1980) 509–516.
[2] T.J. Richmond, J.T. Finch, B. Rusliton, D. Rhodes, A. Klug, Structure of the nucleosome core particle at 7 Å resolution, Nature 311 (1984) 532–537.
[3] D.A. Davey, D.F. Sargent, K. Luger, A.W. Maeder, T.J. Richmond, Solvent mediated interactions in the structure of the nucleosome core particle at 1.9 Å resolution, J. Mol. Biol. 319 (2002) 1097–1113.
[4] K. Luger, A.W. Mäder, R.K. Richmond, D.F. Sargent, T.J. Richmond, Crystal structure of the nucleosome core particle at 2.8 Å resolution, Nature 389 (1997) 251–260.
[5] T.E. Shrader, D.M. Crothers, Artificial nucleosome positioning sequences, Proc. Natl. Acad. Sci. USA 86 (1989) 7418–7422.
[6] T.E. Shrader, D.M. Crothers, Effects of DNA sequence and histone–histone interactions on nucleosome placement, J. Mol. Biol. 216 (1990) 69–84.
[7] J.S. Godde, A.P. Wolffe, Nucleosome assembly on CTG triplet repeats, J. Biol. Chem. 271 (1996) 15222–15229.
[8] J.S. Godde, S.U. Kass, M.C. Hirst, A.P. Wolffe, Nucleosome assembly on methylated CGG triplet repeats in the fragile X mental retardation gene 1 promoter, J. Biol. Chem. 271 (1996) 24325–24328.
[9] Y. Wang, R. Gellibolian, M. Shimizu, R.D. Wells, J. Griffith, Long CCG triplet repeat blocks exclude nucleosomes: a possible mechanism for the nature of fragile sites in chromosomes, J. Mol. Biol. 263 (1996) 511–516.
[10] Y. Wang, J. Griffith, The $[(G/C)_3NN]_n$ motif: a common DNA repeat that excludes nucleosomes, Proc. Natl. Acad. Sci. USA 93 (1996) 8863–8867.
[11] H.R. Widlund, H. Cao, S. Simonsson, et al., Identification and characterization of genomic nucleosome-positioning sequences, J. Mol. Biol. 267 (1997) 807–817.
[12] S. Cacchione, M.A. Cerone, M. Savino, In vitro low propensity to form nucleosomes of four telomeric sequences, FEBS Lett. 400 (1997) 37–41.
[13] P.T. Lowary, J. Widom, New DNA sequence rules for high affinity binding to histone octamer and sequence-directed nucleosome positioning, J. Mol. Biol. 276 (1998) 19–42.
[14] L. Rossetti, S. Cacchione, M. Fuà, M. Savino, Nucleosome assembly on telomeric sequences, Biochemistry 37 (1998) 6727–6737.
[15] M. Del Cornò, P. De Santis, B. Sampaolese, M. Savino, DNA superstructural features and nucleosomal organization on the two centromers of *Kluyveromyces lactis* chromosome 1 and *Saccharomyces cerevisiae* chromosome 6, FEBS Lett. 431 (1998) 66–70.
[16] H. Cao, H.R. Widlund, T. Simonsson, M. Kubista, TGGA repeats impair nucleosome formation, J. Mol. Biol. 281 (1998) 253–260.
[17] D.J. Fitzgerald, J.N. Anderson, Unique translational positioning of nucleosomes on synthetic DNAs, Nucleic Acids Res. 26 (1998) 2526–2535.
[18] D.J. Fitzgerald, J.N. Anderson, DNA distortion as a factor in nucleosome positioning, J. Mol. Biol. 293 (1999) 477–491.
[19] I. Filesi, S. Cacchione, P. De Santis, L. Rossetti, M. Savino, The main role of the sequence-dependent DNA elasticity in determining the free energy of nucleosome formation on telomeric DNAs, Biophys. Chem. 83 (1999) 223–237.
[20] S. Mattei, B. Sampaolese, P. De Santis, M. Savino, Nucleosome organization on *Kluyveromyces lactis* centromeric DNAs, Biophys. Chem. 97 (2002) 173–187.
[21] S. Cacchione, J.L. Rodriguez, R. Mechelli, L. Franco, M. Savino, Acetylated nucleosome assembly on telomeric DNAs, Biophys. Chem. 104 (2003) 381–392.
[22] S. Satchwell, H.R. Drew, A.A. Travers, Sequence periodicities in chicken nucleosome core DNA, J. Mol. Biol. 191 (1986) 659–675.
[23] J.D. McGhee, G. Felsenfeld, Nucleosome structure, Annu. Rev. Biochem. 49 (1980) 1115–1156.
[24] H.R. Drew, A.A. Travers, DNA bending and its relation to nucleosome positioning, J. Mol. Biol. 186 (1985) 773–790.
[25] A.A. Travers, A. Klug, The bending of DNA in nucleosomes and its wider implications, Philos. Trans. R. Soc. Lond. B Biol. Sci. 317 (1987) 537–561.
[26] K.E. van Holde, The nucleosome, in: A. Rich (Ed.), Chromatin, Springer, New York, 1988, pp. 213–276.
[27] J. Widom, Toward a unified model of chromatin folding, Annu. Rev. Biophys. Chem. 18 (1989) 365–395.
[28] T.A. Blank, P.B. Becker, The effect of nucleosome phasing sequences and DNA topology on nucleosome spacing, J. Mol. Biol. 260 (1996) 1–8.
[29] A. Flaus, K. Luger, S. Tan, T.J. Richmond, Mapping nucleosome position at single base-pair resolution by using site-directed hydroxyl radicals, Proc. Natl. Acad. Sci. USA 93 (1996) 1370–1375.
[30] C. Anselmi, G. Bocchinfuso, P. De Santis, M. Savino, A. Scipioni, Dual role of DNA intrinsic curvature and flexibility in determining nucleosome stability, J. Mol. Biol. 286 (1999) 1293–1301.
[31] C. Anselmi, G. Bocchinfuso, P. De Santis, M. Savino, A. Scipioni, A theoretical model for the prediction of sequence-dependent nucleosome thermodynamic stability, Biophys. J. 79 (2000) 601–613.

[32] H.R. Drew, R.E. Dickerson, Structure of a B-DNA dodecamer. III. Geometry of hydration, J. Mol. Biol. 151 (1981) 535–556.
[33] F. Fack, V. Sarantoglou, Curved DNA fragments display retarded elution upon anion exchange HPLC, Nucleic Acid Res. 19 (1991) 4181–4188.
[34] E. Liepinsh, G. Otting, K. Wuthrich, NMR observation of individual molecules of hydration water bound to DNA duplexes: direct evidence for a spine of hydration water present in aqueous solution, Nucleic Acid Res. 20 (1992) 4549–4553.
[35] H.M. Berman, Hydration of DNA: take 2, Curr. Opin. Struct. Biol. 4 (1994) 345–350.
[36] X. Shui, L. McFail-Isom, G.G. Hu, L.D. Williams, The B-DNA dodecamer at high resolution reveals a spine of water on sodium, Biochemistry 37 (1998) 8341–8355.
[37] X. Shui, C.C. Sines, L. McFail-Isom, D. VanDerveer, L.D. William, Structure of the potassium form of CGCGAATTCGCG: DNA deformation by electrostatic collapse around inorganic cations, Biochemistry 37 (1998) 16877–16887.
[38] L. McFail-Isom, C.C. Sines, L.D. William, DNA structure: cations in charge?, Curr. Opin. Struct. Biol. 9 (1999) 298–308.
[39] N.V. Hud, V. Sklenar, J. Feigon, Localization of ammonium ions in the minor groove of DNA duplexes in solution and the origin of DNA A-tract bending, J. Mol. Biol. 286 (1999) 651–660.
[40] P.A. Kitchin, V.A. Klein, K.A. Ryan, et al., A highly bent fragment of *Crithidia fasciculata* kinetoplast DNA, J. Biol. Chem. 261 (1986) 11302–11309.
[41] J. Griffith, M. Bleyman, C.A. Rauch, P.A. Kitchin, P.T. Englund, Visualization of the bent helix in kinetoplast DNA by electron microscopy, Cell 46 (1986) 717–724.
[42] B. Revet, A. Fourcade, Short unligated sticky ends enable the observation of circularised DNA by atomic force and electron microscopies, Nucleic Acids Res. 26 (1998) 2099–2104.
[43] A. Scipioni, C. Anselmi, G. Zuccheri, B. Samorì, P. De Santis, Sequence-dependent DNA curvature and flexibility from scanning force microscopy images, Biophys. J. 83 (2002) 2408–2418.
[44] A. Scipioni, G. Zuccheri, C. Anselmi, A. Bergia, B. Samorì, P. De Santis, Sequence-dependent DNA dynamics by scanning force microscopy time-resolved imaging, Chem. Biol. 9 (2002) 1315–1321.
[45] M.R. Spiegel, Fourier Analysis, McGraw-Hill Book Company, New York, 1974.
[46] C. Anselmi, P. De Santis, R. Paparcone, M. Savino, A. Scipioni, From the sequence to the superstructural properties of DNAs, Biophys. Chem. 95 (2002) 23–47.
[47] B. Sampaolese, A. Bergia, A. Scipioni, et al., Recognition of the DNA sequence by an inorganic crystal surface, Proc. Natl. Acad. Sci. USA 99 (2002) 13566–13570.